

1 **Two Y chromosome-encoded genes determine sex in kiwifruit**

2

3 Takashi Akagi^{1,2,*}, Sarah M. Pilkington³, Erika Varkonyi-Gasic³, Isabelle M. Henry⁴, Shigeo S.
4 Sugano^{2,5}, Minori Sonoda¹, Alana Firl⁴, Mark A. McNeilage³, Mikaela J. Douglas³, Tianchi Wang³,
5 Ria Rebstock³, Charlotte Voogd³, Paul Datson³, Andrew C. Allan^{3,6}, Kenji Beppu⁷, Ikuo Kataoka⁷,
6 Ryutaro Tao¹

7

8 ¹ Graduate School of Agriculture, Kyoto University, Kyoto 606-8502, Japan

9 ² JST, PRESTO, Kawaguchi-shi, Saitama 332-0012, Japan

10 ³ The New Zealand Institute for Plant and Food Research Limited (PFR), Private Bag 92169,
11 Auckland 1142, New Zealand

12 ⁴ Department of Plant Biology and Genome Center, University of California Davis, CA, USA

13 ⁵ R-GIRO, Ritsumeikan University, Shiga 525-8577, Japan

14 ⁶ School of Biological Sciences, University of Auckland, Private Bag 92019, Auckland 1142, New
15 Zealand

16 ⁷ Faculty of Agriculture, Kagawa University, Miki, Kagawa 761-0795, Japan

17

18 *Corresponding author

19 Email: takashia@okayama-u.ac.jp

20 Tel: +81-75-753-6051, Fax: +81-75-753-6497

21

22 [†] Present address: Graduate School of Environmental and Life Science, Okayama University, 700-
23 8530, Okayama, Japan

24

25

26 **ABSTRACT**

27 Dioecy, the presence of male and female individuals, has evolved independently in multiple
28 flowering plant lineages. Although theoretical models for the evolution of dioecy, such as the
29 “two-mutation” model, are well established, little is known about the specific genes determining
30 sex and their evolutionary history. Kiwifruit, a major tree crop consumed worldwide, is a
31 dioecious species. In kiwifruit, we had previously identified a Y-encoded sex-determinant
32 candidate gene acting as the suppressor of feminization (SuF), named *Shy Girl* (*SyGI*). Here, we
33 identified a second Y-encoded sex-determinant that we named *Friendly boy* (*FrBy*), which
34 exhibits strong expression in tapetal cells. Gene-editing and complementation analyses in
35 *Arabidopsis thaliana* and *Nicotiana tabacum* indicated that *FrBy* acts for the maintenance of male
36 (M) functions, independently of *SyGI*, and that these functions are conserved across angiosperm
37 species. We further characterized the genomic architecture of the small (< 1 Mb) male specific
38 region of the Y-chromosome (MSY), which harbors only two genes significantly expressed in
39 developing gynoecia and androecia, respectively: *SyGI* and *FrBy*. Resequencing of the genome
40 of a natural hermaphrodite kiwifruit revealed that this individual is genetically male but carries
41 deletion(s) of parts of the Y-chromosome, including *SyGI*. Additionally, expression of *FrBy* in
42 female kiwifruit resulted in hermaphrodite plants. These results clearly indicate that Y-encoded
43 *SyGI* and *FrBy* act independently as the SuF and M factors in kiwifruit, respectively, and provide
44 insight into the evolutionary path leading to a two-factor sex determination system but also a new
45 breeding approach for dioecious species.

46

47 **MAIN TEXT**

48 In flowering plants, hermaphroditism is ancestral and most common, but a minority of
49 plant species have evolved separate sexes (dioecy), in a lineage-specific manner (1-3). Similar to
50 mammals, sexuality in plants is often determined by a heterogametic male system with XY
51 chromosomes, where the Y chromosome is thought to carry one or two male-determining factors

52 (1, 3, 4, 5). Previous analyses of Y chromosome evolution in plants, initially in *Silene latifolia*
53 and *Carica papaya*, have revealed long non-recombining male-specific regions, which encompass
54 many genes (6-8), although the sex-determining genes have not been fully characterized. Recently,
55 Y chromosome-encoded sex determinants have been identified in persimmons (*Diospyros* spp.)
56 and garden asparagus (*Asparagus officinalis*) (9, 10). In persimmons, the Y-encoded pseudogene
57 *OGI* encodes a small-RNA targeting its autosomal counterpart gene, *MeGI*. To the best of our
58 understanding, *OGI* is sufficient for expression of maleness and repression of female development
59 (3, 9, 11). In garden asparagus, two Y-encoded factors, named *SOFF* and *aspTDF*, act
60 independently to suppress gynoecium and promote androecium development, respectively (10).
61 The asparagus observation is consistent with a previously proposed theoretical framework, called
62 the “two-mutation model” (12, 13), while the persimmon case is not. This model proposes that
63 evolution from an ancestral hermaphrodite could occur if females carried a mutated (non-
64 functional) version of a male promoting factor (M) on the proto-X chromosome, resulting in
65 establishment of gynodioecy. A second mutation, a gain-of function suppressor of feminization
66 (SuF) on the proto-Y chromosome would then establish males. Together, these sex-determining
67 mutations may, if closely linked, define a genome region resembling an XY chromosome pair or
68 sex-linked genome region (13). Still, the evolutionary pathways governing the transitions into
69 dioecy are poorly understood because only a few examples have been characterized to date.

70 Kiwifruit, a major fruit crop consumed worldwide, belongs to the genus *Actinidia*, in
71 which most species are dioecious (14). The sexuality in kiwifruit is genetically controlled by a
72 heterogametic male system (i.e., XY system). A Y-encoded cytokinin response regulator, named
73 *Shy Girl* (*SyGI*), acts as one of the two putative sex determinants, the suppressor of female
74 development (Su^F) (15). The other sex determinant, the putative male promoting factor (M) has
75 not been identified. Although the establishment of SuF in *Actinidia* is estimated to have occurred
76 approximately 20-myra (15) and predated the divergence of the *Actinidia* species, kiwifruit still
77 carries incipient and homomorphic sex chromosomes, including a small sex-determining region

78 (15-17). Recent breeding has derived some hermaphroditic and neuter individuals in *A. deliciosa*,
79 which constitute an additional resource for the identification of a second sex determinant in
80 kiwifruit. Here, we attempted to identify the male promoting sex determinant (M factor), by fine
81 assessment of the genes located on the male-specific region of the Y-chromosome (MSY), and
82 identification of genes differentially expressed between male and female at an early stage of
83 tapetum differentiation. The function of the M factor was validated in model plants and in
84 kiwifruit, resulting in the first development of an artificial hermaphrodite crop from a dioecious
85 individual. Finally, we further assessed the evolution of the two sex determinants on the Y-
86 chromosome, unveiling transitions into and out of dioecy in kiwifruit.

87

88 Previously, genomic sequencing reads from F1 sibling trees derived from an
89 interspecific cross, *A. rufa* sel. Fuchu × *A. chinensis* sel. FCM1 were used to identify and assemble
90 the potential male specific region of the Y chromosome (MSY) of *A. chinensis* (15). The 249
91 resulting contigs, totaling approximately 0.5Mb in length, contained Y-specific sequences with
92 perfect co-segregation with the plants' sex, and included 61 hypothetical genes (15). In kiwifruit,
93 androecia differentiation between males and females is observed during tapetum degeneration
94 (stage 3-4 in Fig. S1) (15, 18, 19). To identify candidate male promoting (M) factors within the
95 MSY, we conducted mRNA-Seq analyses on developing anthers (5 males and 5 females) before
96 tapetum degeneration ("stage 1-2" in Fig. S1) from the F1 population described above. The
97 mRNA-Seq reads were mapped to the 61 hypothetical candidate genes. Only one of them
98 exhibited male-specific expression (RPKM > 1). This gene included a fasciclin domain, which
99 are typically involved in cell adhesion (Table S1). This fasciclin-like gene was named "*Friendly*
100 *Boy (FrBy)*", as a potential counterpart of the Su^F sex determinant, *Shy Girl (SyGI)*. *FrBy* is nested
101 within the monophyletic MTR1 family (Fig. 1a). In rice, MTR1 contributes to tapetum
102 degradation via programmed cell death (PCD), resulting in male fertility (20). The kiwifruit *FrBy*
103 and its orthologs in *Nicotiana tabacum* (FAS1 domain protein), *Arabidopsis thaliana*

104 (AT1G30800) and rice (*Oriza sativa*, MTR1), showed no significant differentiation according to
105 site-branch-specific evolutionary rate analysis against the other branches (Fig. 1b), suggesting
106 conserved protein function. The presence of the *FrBy* gene was male-specific in a wide variety of
107 *Actinidia* species (Fig. 1c). The expression of *FrBy* was specific to early developing androecia
108 (Fig. 1d-e). Tapetum cell-specific qRT-PCR using laser capture microdissection (Supplemental
109 Figure S2) and *in situ* RNA hybridization analysis (Fig. 1f-h) both indicated that *FrBy* expression
110 in androecia was confined to tapetal cells in stage 1-2 and possibly to meiocyte or tetrads. This is
111 consistent with previous observations of MTR1 in rice (Tan et al. 2012) and with its putative
112 function to contribute to tapetum degradation following PCD in kiwifruit (Supplemental Fig. S1
113 and S3) (19). Differentially expressed genes (DEGs) in male and female anthers (Supplemental
114 Table S2, Figure S4) were also consistent with the potential function of *FrBy*. We identified 538
115 DEGs (FDR < 0.1) when analyzing transcriptome data from developing anthers (as described
116 above). In those 538 DEGs, GO terms involving PCD and phosphorylation signals were highly
117 enriched (Supplemental Table S3). Not only PCD, but abundant phosphorylation signals are
118 indispensable for proper tapetum maturing and degradation (21-23). Furthermore, an ortholog of
119 *Tapetal Development and Function 1 (TDF1)* or *MYB35*, a key gene in tapetum maturation in
120 *Arabidopsis* (Zhu et al. 2008) and one of the two sex determinants in dioecious garden asparagus
121 (10, 24, 25), was detected as one of the male-biased DEGs in kiwifruit, although this gene
122 (Acc30672.1) was not located within the MSY (Supplementary Table S2, Figure S5).

123 To investigate the function of *FrBy*, we first used the CRISPR/Cas9 gene editing system
124 in two distantly related model plants, *Arabidopsis thaliana* and *Nicotiana tabacum* (Supplemental
125 Table S4). Although the *Arabidopsis* genome includes three paralogs of *FrBy*, only one,
126 AT1G30800, was in the cluster which was conserved across the *Brassicaceae* species (Fig. 1a).
127 In *Arabidopsis*, the AT1G30800-null lines (Supplemental Figure S6) were self-sterile, with low
128 pollen germination rates (Fig. 2g), but could successfully produce seed after being crossed to
129 control male plants (Fig. 2a-e). The null line showed substantial delay in tapetal layer degradation

130 (Supplemental Fig. S7), which is consistent with the development of female kiwifruit plants (Fig.
131 S1) (18, 19). On the other hand, the lack of AT1G30800 had no significant effect on female
132 reproductive function ($P > 0.1$, Supplemental Fig. S8). In *N. tabacum*, knock-out mutation of the
133 *FrBy* ortholog, *FASI* (*fasI*) (Supplemental Figure S9) resulted in male sterility, with substantial
134 reduction in pollen germination rate, and was accompanied by a delay in tapetum degradation.
135 The other organs, including the gynoecium, showed no differentiation compared to the control
136 plants (Fig. 2h-o). The transgenic *N. tabacum* lines expressing the kiwifruit *Su^F* gene, *SyGI*, under
137 the control of native promoter (*pSyGI-SyGI*) exhibited female-sterility (15). Reciprocal crossing
138 using control plants, *pSyGI-SyGI*, and *fasI* indicated that *SyGI* and *FASI* independently promote
139 gynoecium and androecium development, respectively (Fig. 2p). Importantly, male function in a
140 *fasI* null line could be complemented by introduction of the kiwifruit *FrBy* under the control of
141 its native promoter (Fig. 2q-r, Supplemental Figure S10), indicating that *FrBy* can act to maintain
142 male fertility via proper tapetum degradation in *N. tabacum*. These results all suggest that *FrBy*
143 is likely to be the male promoting factor, and that the two sex determining genes, *SyGI* and *FrBy*
144 work independently for female and male fertility, respectively, in kiwifruit. Furthermore, our
145 phylogenetic and evolutionary analyses indicated that the function of this fasciclin-like
146 monophyletic gene is highly conserved across angiosperm species.

147 Reference genome sequences for kiwifruit have been assembled from female (2A+XX)
148 cultivars (26, 27) but the Y chromosome of kiwifruit (or *Actinidia* spp.) has not been sequenced
149 to date. Here, we constructed the whole genome reference sequence of a male cultivar, Soyu,
150 which is one of the main pollinizers used in Japan. The sequences were assembled using 10X
151 Genomics Supernova v1.2.2, which is based on a long haploblocking method suitable for
152 assembly of highly heterozygous diploid genomes (28). Downstream genomic analysis for the
153 Soyu cultivar was conducted on the "pseudohaploid" version of the whole genome assembly. The
154 drafted genome sequence covered ca 710Mb which corresponds to 94% of the estimated size of
155 kiwifruit genome (758 Mb) (Hopping, 1994, Huang 2013), with $N50 = ca$ 318kb for scaffolds

156 (Supplemental Table S5). The genomic short-read sequences were generated from large DNA
157 molecules partitioned and barcoded using the Gel Bead in Emulsion (GEM) microfluidic method
158 of 10X Genomics (28). Thus, the information present in the GEM barcodes anchored to the
159 assembled contigs reflect their physical distance, in which proximal contig pairs often share the
160 same GEM barcodes. GEM barcodes were extracted from read pairs and linkage information was
161 assigned using a custom script. To construct longer scaffolds within the MSY, we first identified
162 9 scaffolds, which together spanned 1.43 Mb, and contained ca 87% of the Y-specific contigs
163 previously assembled (15) (Supplemental Table S6). To organize these scaffolds relative to each
164 other, we applied DelMapper (6), an approach that employed the traveling salesman problem
165 (TSP), used in radiation hybrid mapping of mammalian chromosomes (29, 30) or deletion
166 mapping of Y-chromosome in dioecious *Silene latifolia* (6). Using this method, 8 of the 9
167 scaffolds were successfully organized. In this new assembled super-scaffold, the two sex
168 determinants, *SyGI* and *FrBy*, are located on adjacent scaffolds, at an estimated distance of ca
169 500kb (Fig. 3a, Supplemental Figure S11). Mapping of genomic reads from male and female
170 individuals in the KE population (15) indicated that a ~800-kb region enriched in male-specific
171 sequences (putative MSY) was located at the center of this assembled super-scaffold (Fig. 3a).
172 The putative MSY includes the two sex determinants and highly repetitive sequences, which is
173 consistent with the structure of MSY in other plants or animals (10, 31). The putative
174 pseudoautosomal region (PAR) appears to be single copy and exhibited no substantial gender-
175 bias, and mostly flanked the putative MSY, although some PAR-like sequences were also located
176 inside the putative MSY (Fig. 3a). In this super-scaffold, 145 genes were predicted using
177 AUGUSTUS (32), and 30 of these genes were fully male-specific (Fig. 3b-c, Supplemental Table
178 S7). Of the 30 male-specific genes, only *SyGI* and *FrBy* were substantially expressed (RPKM >
179 1) in carpel and anther, respectively (Fig. 3d-e, Supplemental Table S8), based on transcriptome
180 information from the KE population (Akagi et al. 2018 for carpel) (15). These data support the
181 hypothesis that they are the two factors determining sexuality in kiwifruit.

182 We further corroborated the role of these two sex determinants in two ways. Breeding
183 programs have generated a few hermaphrodite accessions in hexaploid *A. deliciosa* (33). We
184 sequenced one of them, the KH-line (Supplementary Table S9), which was thought to be a Y-
185 dependent (or possibly X-dependent) hermaphrodite (6A+XXXXXY^h or 6A+XXXXXX^h,
186 Supplementary Figure S12). Mapping of the KH and control *A. deliciosa* [male cv. Matua
187 (6A+XXXXXY)] genomic reads to the Y-chromosomal scaffolds described above (Fig. 3)
188 demonstrated that the KH-line carries the *FrBy* gene, but not the *SyGI* gene, either through one
189 or several long deletion(s), including the loss of *SyGI*, or through gain of *FrBy* on the X
190 chromosome from recombination with the Y chromosome (Figure 4a, Supplementary Figure S13).
191 Consistent with this result, *SyGI* could not be amplified in the KH-line, while *FrBy* could (Figure
192 4b). This suggested that loss of *SyGI* (the Su^F) in the Y, or gain of *FrBy* in the X, resulted in a
193 natural hermaphrodite line (Figure 4c). Next, we set out to develop hermaphrodite kiwifruit
194 artificially, as well as to further validate the *FrBy* function. We introduced the *FrBy* ORF under
195 the control of its native promoter (*pFrBy-FrBy*) into a “rapid flowering” *A. chinensis* female cv.
196 Hort16A. In this line, the *CENTRORADIALIS* (*CEN*) genes have been truncated by gene-editing,
197 resulting in lines that bypass the long juvenile phase (*ca* 3-4 years) and flower precociously (34).
198 As anticipated, the *pFrBy-FrBy* lines, which flowered 4 months after regeneration, were
199 hermaphroditic, exhibiting restored androecium function. These produced fruits including fertile
200 seeds after self-pollination (Fig. 4d-h, Supplementary Table S10). Pollen tubes from the *pFrBy-*
201 *FrBy* lines grew similarly to those from male accessions, in contrast to the control lines (Figure
202 4g-i, Supplementary Figure S14). These results clearly indicated that *FrBy* acts as the M factor in
203 kiwifruit sex determination. They also provide valuable insight into new breeding approaches for
204 dioecious species.

205

206 Taken together, our results are consistent with the following evolutionary path for the
207 transition from hermaphroditism to dioecy in *Actinidia*, based on two tightly linked genes within

208 a small MSY: loss-of-function of *FrBy* established a proto-X chromosome, while lineage-specific
209 gain-of-function in *SyGI* (15) derived a dominant suppressor of gynoecium development,
210 establishing a proto-Y chromosome (Figure 5). This evolutionary process and the predicted
211 function of the determinants are consistent with the “two-mutation model” (12, 13). This proposed
212 evolutionary history of *SyGI* and *FrBy* is also consistent with those of the two-locus type sex
213 determinants in *Asparagus* or *Phoenix* (10, 35), although the specific function of these sex-
214 determinants are different. The putative SuF genes, *SOFF* for *Asparagus* and *LOGI*-like for
215 *Phoenix*, were established by lineage-specific gene duplication/translocation on the Y
216 chromosome; while the putative M genes, *MYB35 (TDF1)* for *Asparagus* and *CPY703/GPAT3*
217 for *Phoenix* were lost from the X chromosomes. Within the order Ericales, kiwifruit (*Actinidia*)
218 evolved these Y-encoded sex determinants while persimmons (*Diospyros*), evolved a single sex
219 determinant on the Y chromosome, *OGI*, which encodes small-RNAs repressing an autosomal
220 feminizing gene, *MeGI* (9, 36). Despite their different specific functions, *SyGI* in kiwifruit and
221 *OGI* in persimmon both act as dominant suppressors and were both derived from lineage-specific
222 duplications, suggesting evolutionary consistency in how the diverse sex determination systems
223 have evolved in angiosperms.

224

225 REFERENCES

- 226 1. Ming, R., Bendahmane, A. & Renner, S. S. Sex chromosomes in land plants. *Ann. Rev. Plant*
227 *Biol.* **62**, 485–514 (2011).
- 228 2. Renner, SS. The relative and absolute frequencies of angiosperm sexual systems: Dioecy,
229 monoecy, gynodioecy, and an updated online database. *Am. J. Bot.* **101**, 1588–1596 (2014).
- 230 3. Henry, I. M., Akagi, T., Tao, R. & Comai, L. One hundred ways to invent the sexes:
231 theoretical and observed paths to dioecy in plants. *Annu Rev Plant Biol.* **69**, 553-575 (2018).
- 232 4. Charlesworth, D. Plant sex chromosome evolution. *J. Exp. Bot.* **64**, 405-420 (2013).
- 233 5. Charlesworth, D. Plant contributions to our understanding of sex chromosome evolution. *New*

- 234 *Phytol.* **208**, 52-65 (2015).
- 235 6. Kazama, Y. *et al.* A new physical mapping approach refines the sex-determining gene
236 positions on the *Silene latifolia* Y-chromosome. *Sci. Rep.* **6**, 18917 (2016).
- 237 7. Liu, Z. *et al.* A primitive Y chromosome in papaya marks incipient sex chromosome evolution.
238 *Nature* **427**, 348-352 (2004).
- 239 8. Wang, J. *et al.* Sequencing papaya X and Y^h chromosomes reveals molecular basis of incipient
240 sex chromosome evolution. *Proc. Natl. Acad. Sci. U. S. A.* **109**, 13710–13715 (2012).
- 241 9. Akagi, T., Henry, I. M., Tao, R. & Comai, L. A Y-chromosome-encoded small RNA acts as a
242 sex determinant in persimmons. *Science* **346**, 646–650 (2014).
- 243 10. Harkess, A. *et al.* The asparagus genome sheds light on the origin and evolution of a young Y
244 chromosome. *Nat. Commun.* **8**, 1279.
- 245 11. Akagi, T. *et al.* Epigenetic regulation of the sex determination gene *MeGI* in polyploid
246 persimmon. *Plant Cell*, **28**, 2905-2915 (2016).
- 247 12. Westergaard, M. The mechanism of sex determination in dioecious flowering plants. *Adv.*
248 *Genet.* **9**, 217–281 (1958).
- 249 13. Charlesworth, B. & Charlesworth, D. A model for the evolution of dioecy and gynodioecy.
250 *Amer. Nat.* **112**, 975-997 (1978).
- 251 14. Datson, P. M. & Ferguson, A. R. *Actinidia*. Wild Crop Relatives: Genomic and Breeding
252 Resources, Tropic. Subtropic. Fruits, ed Kole C (Springer, Berlin Heidelberg), pp 1-20 (2011).
- 253 15. Akagi, T. *et al.* A Y-encoded suppressor of feminization arose via lineage-specific duplication
254 of a cytokinin response regulator in kiwifruit. *Plant Cell* **30**, 780-795 (2018).
- 255 16. Fraser, L. G. *et al.* A gene-rich linkage map in the dioecious species *Actinidia chinensis*
256 (kiwifruit) reveals putative X/Y sex-determining chromosomes. *BMC Genom.* **10**, 102 (2009).
- 257 17. Zhang, Q. *et al.* High-density interspecific genetic maps of kiwifruit and the identification of
258 sex-specific markers. *DNA Res.* **22**, 367-375 (2015).

- 259 18. Messina, R. Microsporogenesis in male-fertile cv. Matua and male-sterile cv. Hayward of
260 *Actinidia deliciosa* var. *deliciosa* (Kiwifruit). *Adv. Hort. Sci.* **7**, 77-81 (1993).
- 261 19. Falasca, G. et al. Tapetum and middle layer control male fertility in *Actinidia deliciosa*. *Ann.*
262 *Bot.* **112**, 1045-1055 (2013).
- 263 20. Tan, H., Liang, W., Hu, J. & Zhang, D. MTR1 encodes a secretory fasciclin glycoprotein
264 required for male reproductive development in rice. *Dev Cell* **22**, 1127-1137 (2012).
- 265 21. Zhang, D. & Yang, L. Specification of tapetum and microsporocyte cells within the anther.
266 *Curr. Opin. Plant Biol.* **17**, 49-55 (2014).
- 267 22. Ye, J. et al. Proteomic and phosphoproteomic analyses reveal extensive phosphorylation of
268 regulatory proteins in developing rice anthers. *Plant J.* **84**, (2015).
- 269 23. Ye, J. et al. Abundant protein phosphorylation potentially regulates Arabidopsis anther
270 development. *J. Exp. Bot.* **67**, 4993-5008 (2016).
- 271 24. Tsugama, D. et al. A putative MYB35 ortholog is a candidate for the sex-determining genes
272 in *Asparagus officinalis*. *Sci. Rep.* **7**, 41497 (2017).
- 273 25. Murase, K. et al. MYB transcription factor gene involved in sex determination in *Asparagus*
274 *officinalis*. *Genes Cells* **22**, 115-123 (2017).
- 275 26. Huang, S. et al. Draft genome of the kiwifruit *Actinidia chinensis*. *Nat. Comm.* **4**, 2640 (2013).
- 276 27. Pilkington, S. M. et al. A manually annotated *Actinidia chinensis* var. *chinensis* (kiwifruit)
277 genome highlights the challenges associated with draft genomes and gene prediction in plants.
278 *BMC Genom.* **19**, 257 (2018).
- 279 28. Weisenfeld, N. I. et al. Direct determination of diploid genome sequences. *Genome Res.* **27**,
280 757-767 (2017).
- 281 29. Ben-Dor, A., Chor, B. & Pelleg, D. RHO - Radiation Hybrid Ordering. *Genome Res.* **10**, 365-
282 378 (2000).

- 283 30. Schäffer, A. A., Rice, E. S., Cook, W. & Agarwala, R. rh_tsp_map 3.0: end-to-end radiation
284 hybrid mapping with improved speed and quality control. *Bioinformatics* **23**, 1156-1158
285 (2007).
- 286 31. Bachtrog, D. *et al.* Sex determination: Why so many ways of doing it? *PLoS Biol.* **12**,
287 e1001899 (2014).
- 288 32. Stanke, M., Steinkamp, R., Waack, S. & Morgenstern, B. AUGUSTUS: a web server for gene
289 finding in eukaryotes. *Nucl. Acids Res.* **32**, 309-312 (2004).
- 290 33. McNeilage, M. A. & Steinhagen, S. Flower and fruit characters in a kiwifruit hermaphrodite.
291 *Euphytica* **101**, 69-72 (1998).
- 292 34. Varkonyi-Gasic, E. *et al.* Mutagenesis of kiwifruit *CENTRORADIALIS*-like genes transforms
293 a climbing woody perennial with long juvenility and axillary flowering into a compact plant
294 with rapid terminal flowering. [Plant Biotechnol J 17, 869-880 \(2019\).](#)
- 295 35. Torres, M. *et al.* Genus-wide sequencing supports a two-locus model for sex-determination
296 in *Phoenix*. *Nat. Comm.* **9**, 3969 (2018).
- 297 36. Yang, H-W. Akagi, T., Kawakatsu, T. & Tao, R. Gene networks orchestrated by *MeGI*: a
298 single-factor mechanism underlying sex determination in persimmon. *Plant J.* **98**, 97-111
299 (2019).
- 300

301 **SUPPLEMENTARY INFORMATION**

302 **Materials and Methods (S1-S11)**

303 **Method S1:** Screening of the expressed candidate sex determinants

304 **Method S2:** Expression profiling in kiwifruit anthers

305 **Method S3:** *in situ* RNA hybridization

306 **Method S4:** Phylogenetic analysis and detection of positive selection

307 **Method S5:** 10X Genomics (Chromium) library construction and genome assembly with
308 Supernova

309 **Method S6:** Anchoring and characterization of the scaffolds surrounding the two sex
310 determinants

311 **Method S7:** Breeding of hermaphrodite kiwifruit

312 **Method S8:** Genomic analysis of hermaphrodite kiwifruit

313 **Method S9:** Construction of vectors

314 **Method S10:** Transformation

315 **Method S11:** Floral phenotyping in transformed plants

316

317 **Accession numbers**

318

319 **Supplemental Figures (S1-S14)**

320 **Supplemental Figure S1:** Transition of anther and definition of the developmental stage

321 **Supplemental Figure S2:** Tapetum cells-specific *FrBy* expression pattern with laser capture
322 microdissection (LCM).

323 **Supplemental Figure S3:** Visualization of programmed cell death in tapetum cells of male and
324 female kiwifruit

325 **Supplemental Figure S4:** Gene expression pattern in male and female anthers

326 **Supplemental Figure S5:** Phylogenetic analysis of TDF1/MYB35-like genes in *Actinidia*

- 327 **Supplemental Figure S6:** Gene disruption of *ATIG30800* in *Arabidopsis* using CRISPR/Cas9
- 328 **Supplemental Figure S7:** Characterization of anther development in *ATIG30800* null line
- 329 **Supplemental Figure S8:** Silique and seed production in *ATIG30800* null line
- 330 **Supplemental Figure S9:** Gene disruption of *FAS1* in *Nicotiana tabacum* using CRISPR/Cas9
- 331 **Supplemental Figure S10:** Complementation of male function in *FAS1* null lines by kiwifruit
- 332 *FrBy*
- 333 **Supplemental Figure S11:** Correspondence between GEM barcodes and the anchored scaffolds
- 334 **Supplemental Figure S12:** Segregation of *FrBy*, in a KH-derived segregating populations.
- 335 **Supplemental Figure S13:** Characterization of the putative KH-specific deletion
- 336 **Supplemental Figure S14:** Cross pollination with p*FrBy*-*FrBy*-induced cv. Hort 16A
- 337
- 338 **Supplemental Tables (S1-S12)**
- 339 **Supplemental Table S1:** 61 hypothetical genes identified in the MSY contigs and their
- 340 expression levels in anther
- 341 **Supplemental Table S2:** List of DEGs between male and female anthers
- 342 **Supplemental Table S3:** GO enrichment analysis in the DEGs between male and female anthers
- 343 **Supplemental Table S4:** Characterization of gene-edited *Arabidopsis* and *N. tabacum* lines
- 344 **Supplemental Table S5:** Summary of the draft genome assembly in cv. Soyu by 10X Genomics
- 345 data
- 346 **Supplemental Table S6:** List of the assembled scaffolds of cv. Soyu anchored by Y-specific
- 347 contigs
- 348 **Supplemental Table S7:** List of genes predicted in the 9 scaffolds anchored by the Y-specific
- 349 contigs
- 350 **Supplemental Table S8:** Expression patterns of the genes predicted in the 9 scaffolds anchored
- 351 by the Y-specific contigs
- 352 **Supplemental Table S9:** Pedigree of the KH line and the segregating population derived from

353 the KH line

354 **Supplemental Table S10:** Phenotypic characterization in p*FrBy*- *FrBy*-induced kiwifruit.

355 **Supplemental Table S11:** List of plant materials.

356 **Supplemental Table S12:** List of primers used in this study.

357

358 **ACKNOWLEDGEMENTS**

359 We thank Dr. Luca Comai (UC Davis Dept. Plant Biology and Genome Center) for technical
360 advice and bioinformatics support, Drs. Yusuke Kazama and Kotaro Ishii (Riken Institute) for
361 technical support for using the DelMapper program, and Niels Nieuwenhuizen and Jane (Lei)
362 Zhang for vector construction. The KE population were originally provided from Kagawa
363 Prefectural Agricultural Experiment Station. Some of this work was performed at the Vincent J.
364 Coates Genomics Sequencing Laboratory at UC Berkeley, supported by NIH S10 OD018174
365 Instrumentation Grant. This work was supported by PRESTO Grant Number JPMJPR15Q1 (to
366 TA) and JPMJPR15Q6 (to SSS) from the Japan Science and Technology Agency (JST), by a
367 Grant-in-Aid for Scientific Research on Innovative Areas No. J16H06471 (to TA) from JSPS,
368 and by the National Science Foundation (NSF) IOS award under Grant No. 1457230 (to IMH)

369

370 **AUTHOR CONTRIBUTION**

371 TA, IK, and RT conceived the study. TA designed the experiments. TA, SMP, EV, SSS, MS, AF,
372 MJD, TW, RR and CV conducted the experiments. TA, SMP, EV, SSS, MS, IMH, and AF
373 analyzed the data, SMP, MAM, PD, ACA, KB, and IK initiated/bred and maintained the plant
374 materials. TA, SMP, EV, and IMH drafted the manuscript. All authors approved the manuscript.

375

376 **AUTHOR INFORMATION**

377 All sequence data generated in the context of this manuscript has been deposited in the appropriate
378 DDBJ database: Illumina reads for gDNAseq and mRNAseq in the Short Read Archives (SRA)

379 database (SRA IDs), the genomic contig sets constructed with 10X Genomics reads were
380 submitted to Genbank (IDs).

381

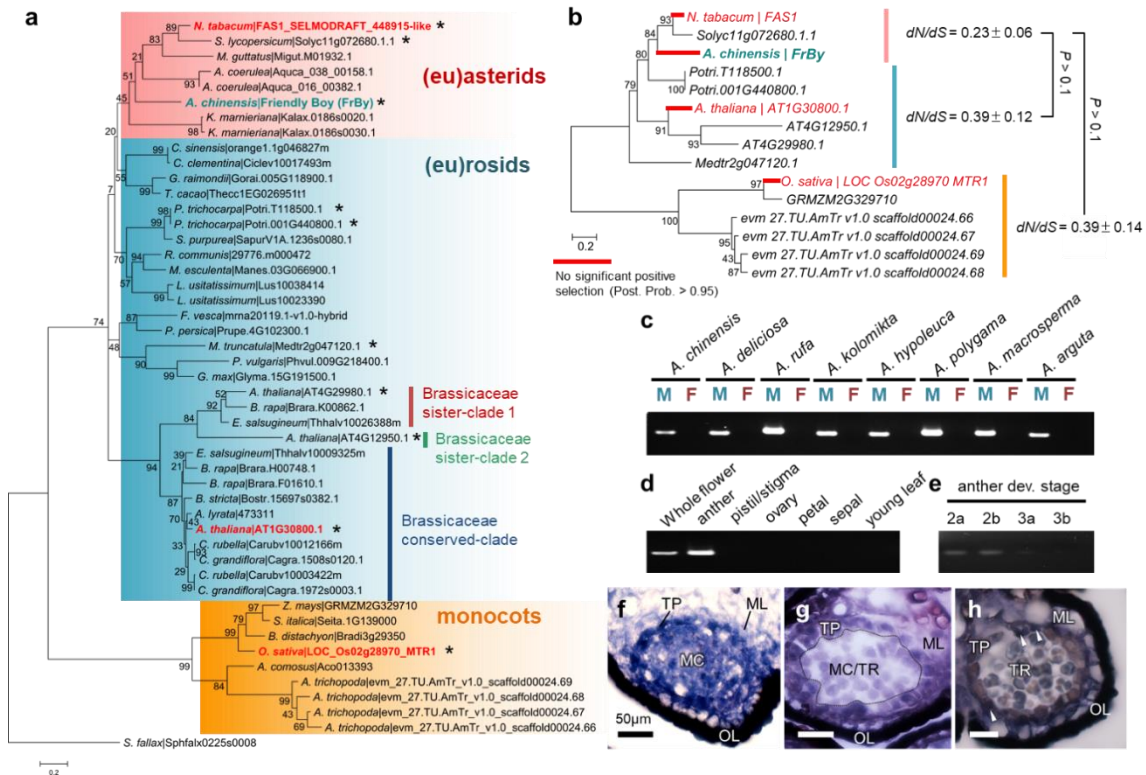
382 Reprints and permissions information is available at www.nature.com/reprints.

383 The authors declare no competing financial interests.

384 Correspondence and requests for materials should be addressed to Takashi Akagi
385 (takashia@okayama-u.ac.jp).

386

387



388

389

390 Figure 1: Identification of the fasciclin-like FrBy as the candidate of the M factor

391 a, Phylogenetic tree of fasciclin-like genes from 32 angiosperm species, including the kiwifruit

392 FrBy (light green). The orthologs from (eu)asterids, (eu)rosids, and monocots constitute three

393 putatively monophyletic clades, shown in red, blue and yellow, respectively. The family

394 Brassicaceae forms three subclades, although only one of them is conserved across the

395 Brassicaceae species. The gene functions of the orthologs written in red have been validated

396 previously (for MTR1 in rice) or in this study (for AT1G30800 for Arabidopsis, FAS1 for

397 Nicotiana tabacum). The orthologs with asterisks were used for further evolutionary analysis in

398 panel (b). **b**, pairwise evolutionary rates (dN/dS) in each clade suggested no protein functional

399 differentiation between these orthologs. No site-branch specific positive selection was detected

400 in red branches, suggesting that protein function and key domains were conserved in MTR1,

401 AT1G30800, FAS1, and kiwifruit FrBy. **c**, PCR analysis specific to FrBy. Male-specificity of

402 FrBy is conserved in a wide variety of *Actinidia* species. M: male, F: female. **d-e**, expression

403 pattern of FrBy. **(d)**, FrBy is expressed specifically in anthers and not on other organs. Within the

404 anthers (e), FrBy is substantially expressed in stage 2a-b, and faintly at stage 3a. **f-h**, RNA *in situ*

405 hybridization using antisense FrBy probe. FrBy is expressed highly in tapetum cells (TP) and

406 meiocyte (MC) at stage 2a **(f)**, in tapetum cells only at stage 2b **(g)**, and faintly in tapetum cells

407 (shown by arrows) at stage 3a **(h)**. These results of RNA *in situ* hybridization were consistent

408 with tapetum-specific expression analysis using laser capture microdissection (Supplemental

409 Figure S2).

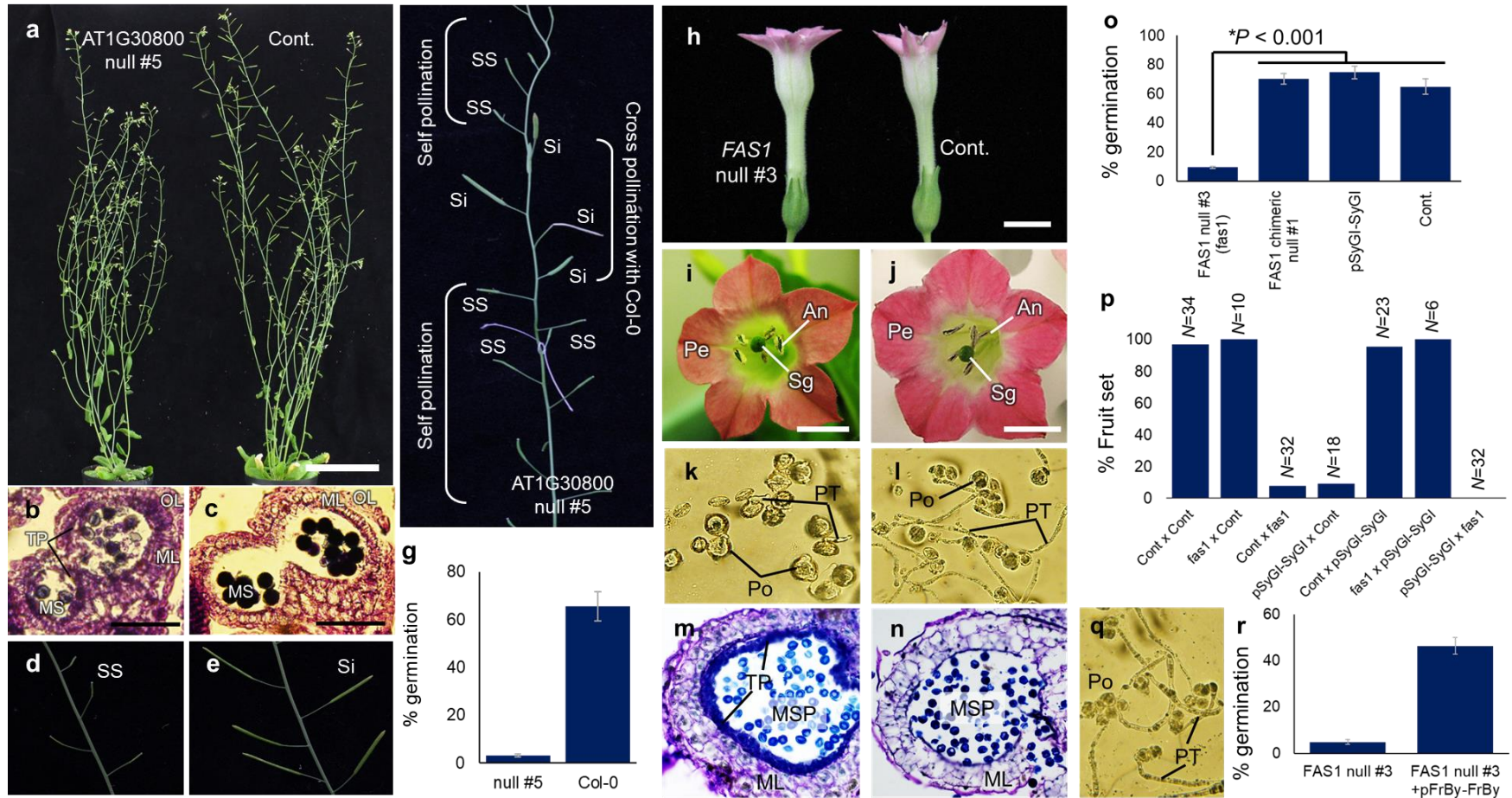


Figure 2: Functional validation of *FrBy* in two model plants.

a-g, A knock-out mutation in the *FrBy* ortholog, *AT1G30800*, resulted in male sterility in Arabidopsis. **a**, phenotype of the *AT1G30800* null mutant #5 and control lines. Developing anthers showed no tapetum degradation in the *AT1G30800* null mutant (**b**), while controls showed complete degeneration of tapetum cells and matured microspore (MS) (**c**). TP: tapetum cells, OL: outer layer, ML: middle layer. **d-e**, reduced seed production

in the *ATIG30800* null mutant (**d**) and control (**e**). SS: sterile silique bearing no seeds, Si: silique. **f**, silique development after self- and cross-pollination of the *ATIG30800* null mutant line #5. Only cross pollination with Col-0 control plants resulted in seeds production. **g**, pollen germination ratios in *ATIG30800* null mutant #5 and #2, and control plants (Col-0). Null mutant #5 mostly lost the ability to produce fertile pollen, and chimeric null mutant #3 showed substantial reduction in pollen fertility. **h-p**, In *N. tabacum*, knock-out mutants of the *FrBy* ortholog, *FASI*, showed male sterility. Whole plant (**h**) and flower organs (**i** for the *FASI* mutant and **j** for control) phenotypes were not different between the *FASI* null mutant and control lines. An: anther, Sg: stigma, Pe: petal. Pollen germination ability was substantially reduced in the *FASI* null mutant (**k**), in comparison to the control lines (**l**). Po: pollen grain, PT: pollen tube. Thick tapetum layers were observed after anther dissection in the microspore stage of the *FASI* null mutant (**m**), while control lines showed complete degradation of tapetum cells (**n**). In comparison to the *FASI* null mutant, the SuF gene, *SyGI*, had no significant effect on pollen germination rate (**o**). Reciprocal crosses with control, *FASI* null, and *SyGI*-expressing lines indicated that *FASI* and *SyGI* act only for male and female functions, respectively (**p**). **q-r**, complementation of male function in *FASI* null, using the kiwifruit *FrBy* gene under the control of its native promoter (*pFrBy-FrBy*). Observation of pollen germination (**q**) and germination ratio (**r**) in *FASI* null mutants transformed with *pFrBy-FrBy*.

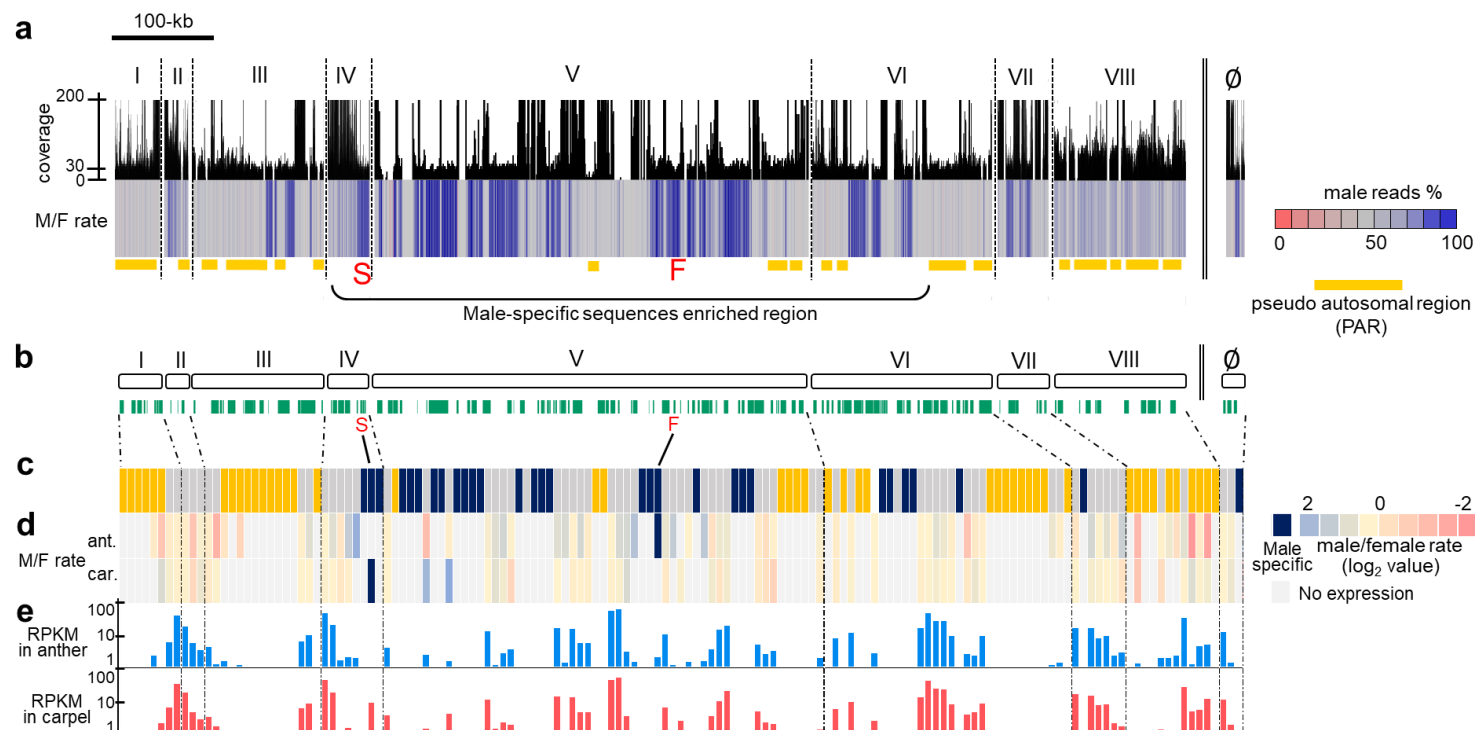


Figure 3. Sequence architecture of the kiwifruit Y chromosome, including the two sex determinants

a, Super-scaffold constituted of anchored 8 contigs (I-VIII) and unanchored one (\emptyset), with coverage of male genomic read (bars) and percentage of male genomic reads (color chart). The coverage from simplex alleles at single sites (or male-specific region with no X-chromosome counterpart) is estimated at 20-23X. Repeated regions, such as transposable elements, were identified as those with high coverage ($>50X$). Putative pseudo-autosomal regions (PAR) were defined as non-repetitive regions with unbiased reads coverage (ca 25-75% male reads), and highlighted with orange bars. *SyGI* (S) and *FrBy* (F) were located on male-specific regions in the middle of the Y-chromosomal contigs. **b**, models of the nine contigs (white bars) and the genes predicted in these contigs (green bars). **c**, male-specificity in the predicted genes in each contig. Genes in male-specific, PAR, and repetitive regions, are shown in blue, orange, and gray, respectively. **d-e**, expression patterns of the predicted genes in each contig. **d**, expression bias between male and female individuals, in anthers (ant.) and carpels (car.). Complete male-specific expression was given in thick blue. **e**, expression levels (RPKM) in anther and carpel. Across the Y-specific genes as given in deep blue, only *FrBy* and *SyGI* were substantially expressed (RPKM > 1) in differentiating anther and carpel, respectively.

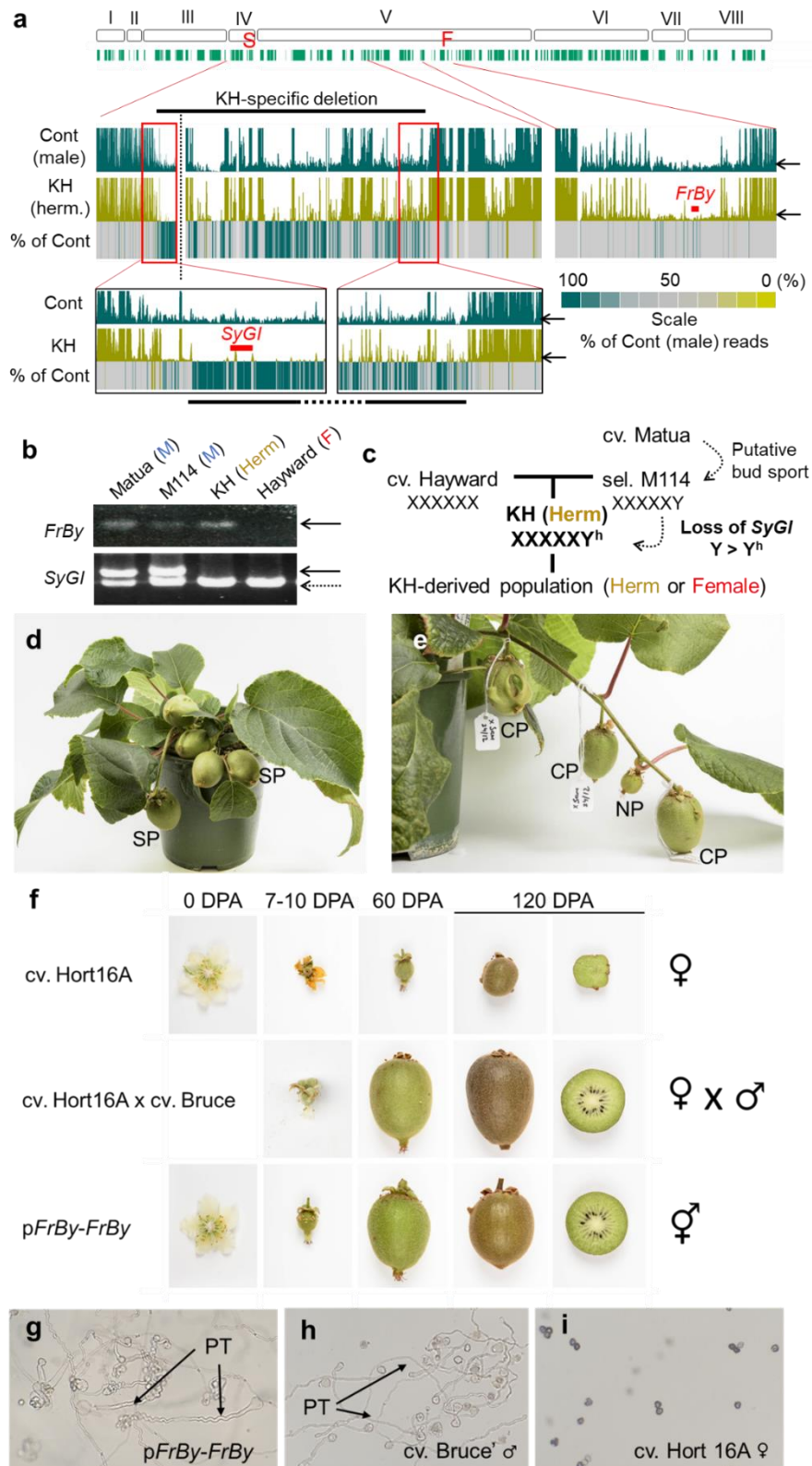


Figure 4. Lost of *SyGI*, or gain of *FrBy* resulted in a natural and synthetic hermaphrodite kiwifruit, respectively

a, Genomic context in the Y-chromosomal contigs, in male cv. Matua (control), and a natural hermaphrodite line, KH. The KH line carries long deletions across contigs IV-V, including *SyGI*.

This was confirmed by PCR analyses (Supplemental Figure S13). The right arm of contig V was conserved in the KH line. Arrows indicated estimated coverage of simplex Y allele. **b**, conservation of *FrBy* and *SyGI* in KH and its parental cultivars/lines, based on the pedigree of the KH lines (as shown in **c**). Solid arrows indicated *FrBy* and *SyGI*. Dotted arrow showed a paralog of *SyGI* with high sequence homology located on an autosome (Akagi et al. 2018). M: male, F: female. *SyGI* is absent specifically in the KH line, while *FrBy* was conserved in both parental males and the KH lines. **c**, pedigree of the KH line and model for the establishment of the *SyGI* null Y^h chromosome. **d-i**, development of hermaphrodite kiwifruit by transformation with *FrBy* under the native promoter (*pFrBy-FrBy*). **d**, The *pFrBy-FrBy* lines showed fertilized fruits with self-pollination (SP) in 120 days post anthesis (DPA). **e**, Control female cv. Hort16A showed unfertilized fruit in non-pollination (NP), while cross-pollination with *pFrBy-FrBy* pollen (CP) resulted in fertilized fruit. **f**, In control female cv. Hort16A (top panels), flowers aborted or developed small parthenocarpic fruit without seeds. In cross pollination of control female and a male cv. Bruce (middle), normal fruits bearing fertile seeds were developed on pollinated cv. Hort16A. In self-pollination of transgenic cv. Hort 16A with *pFrBy-FrBy* (bottom), normal fruits with fertile seeds were developed, comparable to normal female x male. Pollen grains from *pFrBy-FrBy*-induced female cv. Hort16A (**g**) had the ability to grow pollen tubes (PT), as well as from male cv. Bruce (**h**), while pollen grains from control female cv. Hort16A were sterile (**i**).

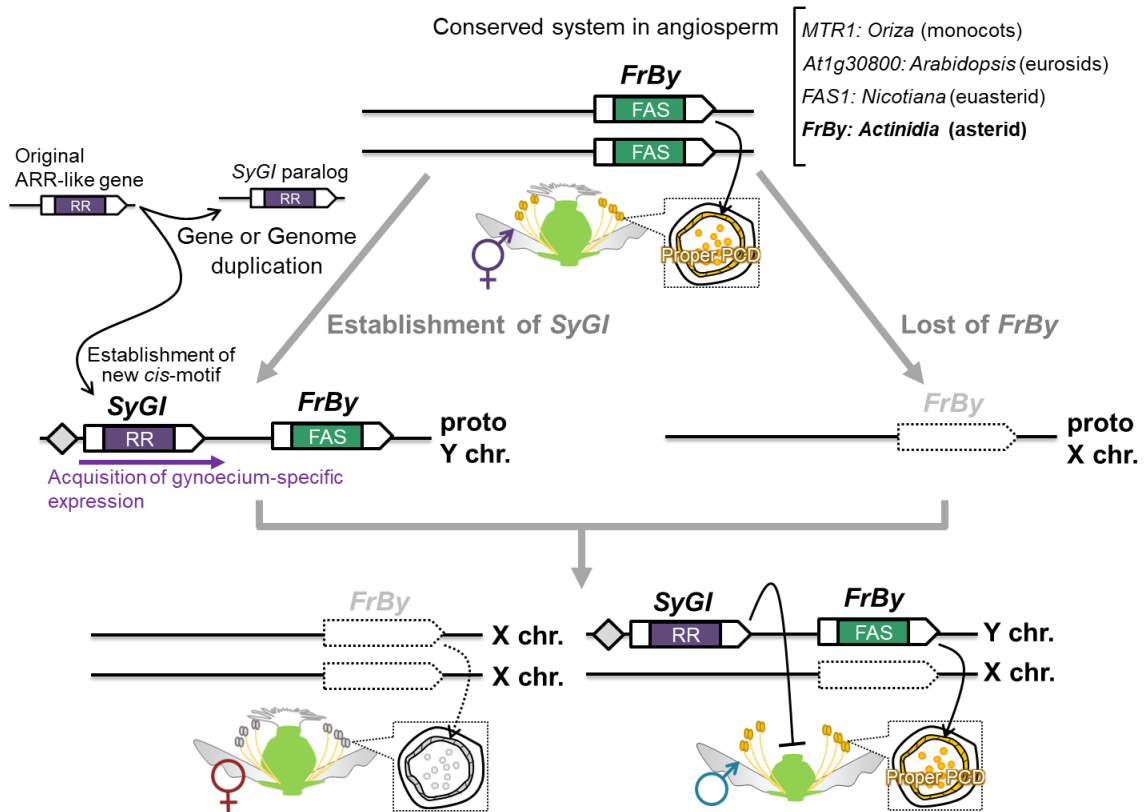


Figure 5: Evolutionary model for the establishment dioecy in *Actinidia*

The putative hermaphrodite ancestor bears an intact *FrBy* ortholog, which carries a function that is conserved across angiosperm. The loss of function in *FrBy* generated a proto X-chromosome, while the gain of function in *SyGI* (15), which occurred next to the intact copy of *FrBy*, resulted in a proto Y-chromosome. Together, these proto X and Y chromosomes evolved to derive the current XY system in the *Actinidia* genus.